

Flame-retardant properties and mechanisms of epoxy thermosets modified with two phosphorus-containing phenolic amines

Peng Wang, Fusheng Yang, Liang Li, Zaisheng Cai

College of Chemistry, Chemical Engineering and Biotechnology, Donghua University, Shanghai 201620,

People's Republic of China

Correspondence to: Z. Cai (E-mail: zshcai@dhu.edu.cn)

ABSTRACT: Two phosphorus-containing phenolic amines, a 9,10-dihydro-9-oxa-10-phosphaphenanthrene-10-oxide (DOPO)-based derivative (DAP) by covalently bonding DOPO and imine (SB) obtained from the condensation of *p*-phenylenediamine with salicylaldehyde, and its analog (AP) via the addition reaction between diethyl phosphite and SB, were used to prepare flame-retardant epoxy resins. The burning behaviors and dynamic mechanical properties of epoxy thermosets were studied by limited oxygen index (LOI) measurement, UL-94 test, and dynamic mechanical analysis. The flame-retardant mechanisms of modified thermosets were investigated by thermogravimetric analysis, Py-GC/MS, Fourier transform infrared, SEM, elemental analysis, and laser Raman spectroscopy. The results revealed that epoxy thermoset modified with DAP displayed the blowing-out effect during UL-94 test. With the incorporation of 10 wt % DAP, the modified thermoset showed an LOI value of 36.1% and V-0 rating in UL-94 test. The flame-retardant mechanism was ascribed to the quenching and diluting effect in the gas phase and the formation of phosphorus-rich char layers in the condensed phase. However, the thermoset modified with 10 wt % AP only showed an LOI value of 25.7% and no rating in UL-94 test, which was possibly ascribed to the mismatching of charring process with gas emission process during combustion. © 2016 Wiley Periodicals, Inc. *J. Appl. Polym. Sci.* **2016**, *133*, 43953.

KEYWORDS: degradation; flame retardance; thermal properties; thermosets

Received 17 January 2016; accepted 15 May 2016

DOI: 10.1002/app.43953

INTRODUCTION

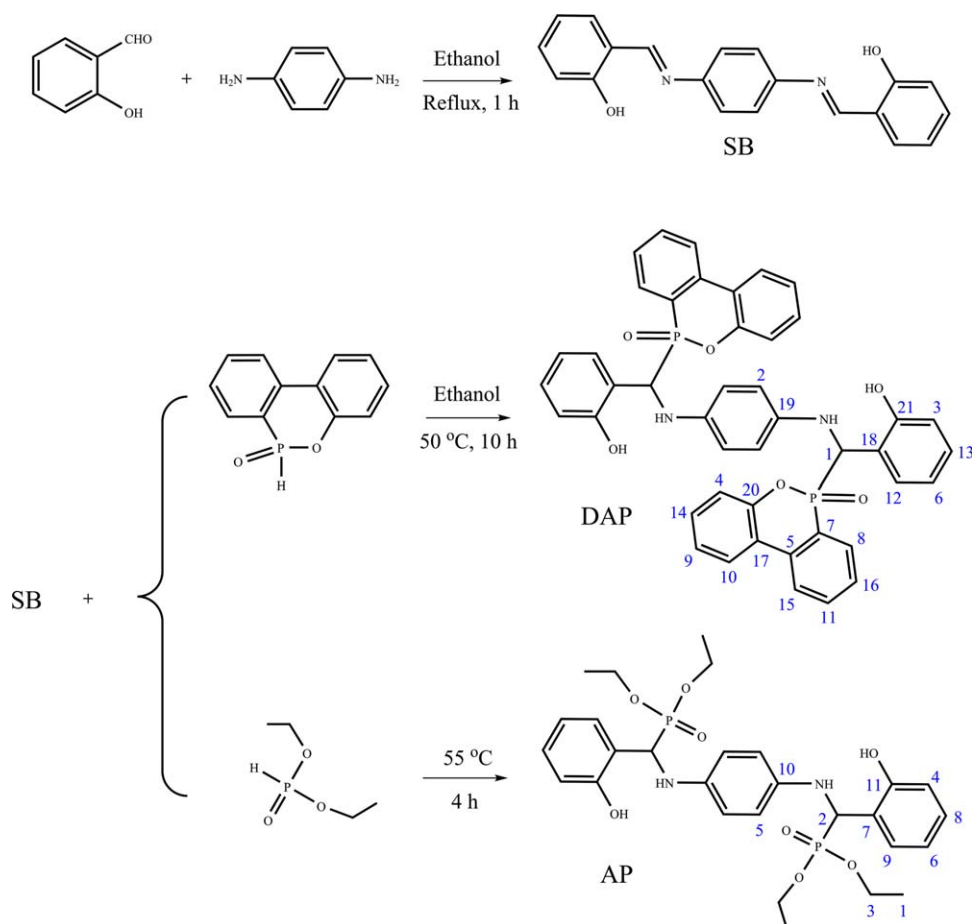
As one of the most prominent thermosetting polymers, epoxy resin has been widely used in adhesives, laminates, composites, molding compounds, surface coating, and microelectronic materials owing to its high tensile strength, good chemical resistance, outstanding adhesive property, low shrinkage in curing, excellent dimensional stability, and superior electrical property.^{1–3} However, just like other polymers, high flammability is one of the main drawbacks of epoxy resin. To meet the strict requirements of industrial fields requiring flame resistance, it is imperative to improve the flame retardancy of epoxy resin.

In the past decades, halogenated compounds are used to endow epoxy resins with flame retardancy because of their effectiveness and affordability. Nevertheless, major problems encountered with this system include the generation of toxic and corrosive fumes during combustion, which are harmful to the human health and environment.^{4,5} Therefore, the usage of halogen-free flame retardants has attracted great attention from both industrial and academic research studies. Phosphorus-based organic compounds have been demonstrated as efficient flame retard-

ants for epoxy resin owing to their outstanding advantages such as high-flame-retardant efficiency and low toxicity.⁶ In the meantime, many excellent studies have indicated that the utilization of other flame-retardant elements, especially nitrogen, would bring about a prominent improvement in the flame-retardant efficiency due to phosphorus–nitrogen synergistic effect.^{7,8}

Recently, 9,10-dihydro-9-oxa-10-phosphaphenanthrene-10-oxide (DOPO) has captured much interest for its great potential to construct phosphorus–nitrogen synergism because of its multiple structural diversification by functionalization. The high reactivity of P–H bond in DOPO can react with a number of electron-deficient compounds containing imine,^{7,9–12} maleimide,^{13,14} phosphazene,^{15,16} triazine,^{6,17} and triazine-trione^{18,19} structures, thus integrating phosphorus and nitrogen element into DOPO-based derivatives. These derivatives, either as reactive curing agents or additives introduced into epoxy matrices, have imparted improved flame retardancy to epoxy resins.

To date, DOPO-based derivatives by the addition of DOPO to imine linkage (DPI), with the secondary amine in the molecular structure, have attracted considerable interest toward researchers.



Scheme 1. Synthetic routes of DAP and AP. [Color figure can be viewed in the online issue, which is available at wileyonlinelibrary.com.]

As flame-retardant co-curing agents, they have endowed epoxy resins with remarkably improved flame retardancy due to phosphorus–nitrogen synergism. Yao and coworkers^{9–11} synthesized a range of DPis, which presented highly flame-retardant effect in cured epoxy resin with 1.0 wt % phosphorus content. Xiong *et al.* synthesized a kind of DPI with triazine group, which imparted improved flame retardancy to epoxy resin. Moreover, the modified epoxy thermoset possessed higher glass transition temperature (T_g) and thermal stability compared to neat thermoset.⁶ Xu *et al.*⁷ reported a flame-retardant epoxy resin modified with a novel DPI, and it showed highly effective flame retardancy with a limiting oxygen index (LOI) value of 39.7% and V-0 rating in UL-94 test at 0.5 wt % phosphorus content. Although the above researches have demonstrated that DPI can notably improve the flame retardancy of epoxy resin at low phosphorus content, the previous researches were focused mainly on the flame-retardant properties of epoxy thermoset. To the best of our knowledge, the flame-retardant mechanism of DPI in epoxy resin has not yet been clarified.

In this work, a DPI (coded as DAP) synthesized according to a previous report¹¹ was used to prepare flame-retardant epoxy resin. To better disclose the flame-retardant mechanism of DAP in epoxy resin, its analog (indicated as AP) was also prepared and used to improve the flame retardancy of epoxy resin. After the burning behaviors of epoxy thermosets were analyzed, the

blowing-out effect observed during combustion and flame-retardant mechanism of epoxy thermosets modified with DAP were investigated particularly. Meanwhile, the reason of inferior flame retardancy for thermoset modified with AP was also studied in detail.

EXPERIMENTAL

Materials

4,4'-Diaminodiphenylmethane (DDM), *p*-phenylenediamine, *N,N*-dimethylformamide (DMF), and ethanol were of reagent grade and purchased from Sinopharm Chemical Reagent Co., Ltd. (Shanghai, China). Salicylaldehyde and diethyl phosphite were obtained from Shanghai Aladdin Chemical Reagent Co., Ltd. (Shanghai, China). DOPO was kindly offered by Jiangyin Hangfeng Technology Co., Ltd. (Jiangsu, China) and recrystallized from ethanol prior to use. Epoxy resin (DGEBA, commercial name: E-44, epoxy value: 0.44 mol/100 g) was provided by Nantong Xingchen Synthetic Material Co., Ltd. (Jiangsu, China).

Syntheses of DAP and AP

The synthetic routes of DAP and AP are illustrated in Scheme 1. The intermediate imine coded as SB was synthesized by a typical condensation reaction. To a 500-mL three-necked round-bottomed flask equipped with a magnetic stirrer and a reflux condenser, *p*-phenylenediamine (0.1 mol, 10.81 g) dissolved in

Table I. Formulations of Epoxy Thermosets

Sample	Composition (g)				DAP (wt %)	AP (wt %)	P (wt %)
	DGEBA	DDM	DAP	AP			
EP	100	21.82	0	0	0	0	0
EP/DAP4	100	20.49	5.02	0	4	0	0.33
EP/DAP7	100	19.44	8.99	0	7	0	0.58
EP/DAP10	100	18.34	13.15	0	10	0	0.83
EP/AP10	100	17.46	0	13.05	0	10	1.05

ethanol (250 mL) was added. The reaction mixture was then increased to 85 °C. Subsequently, salicylaldehyde (0.2 mol, 24.42 g) was added dropwise into the flask within 10 min. The solution was stirred at 85 °C for 1 h. Finally, the orange-red precipitate was filtered, washed with ethanol, and dried at 70 °C for 24 h in a vacuum oven (30.82 g, yield: 97.5%).

The DAP was synthesized according to the literature.¹¹ Specifically, SB (0.05 mol, 15.81 g), DOPO (0.1 mol, 21.60 g), and ethanol (150 mL) were introduced into a 250-mL three-necked round-bottomed flask equipped with a magnetic stirrer and a reflux condenser. The reaction mixture was stirred at 50 °C for 12 h. After that, the reaction mixture was filtered, washed with ethanol, and dried at 70 °C for 24 h in a vacuum oven. The light-yellow solid was recovered (34.66 g, yield: 92.6%). Fourier transform infrared (FTIR; KBr, cm^{-1}): 3359 (N—H); 3172 (O—H); 1594, 1475 (P—C_{Ar}); 1215 (P=O); 1195, 934 (P—O—C_{Ar}). ¹H-NMR (DMSO-*d*₆, δ , ppm): 5.05–5.40 (2H, P—C—H); 5.58–5.77 (1H, —NH—); 5.93–6.10 (1H, —NH—); 6.21–8.33 (14H, Ar-H); 9.39–9.60 (2H, —OH). ¹³C-NMR (DMSO-*d*₆, δ , ppm): 50.1, 51.2 (C₁); 115.0, 115.1 (C₂); 119.4 (C₃); 120.6, 120.8 (C₄); 121.7, 121.9 (C₅); 122.6, 122.7 (C₆); 123.2, 123.8 (C₇); 124.2, 124.4 (C₈); 124.9, 125.1 (C₉); 125.8, 126.0 (C₁₀); 128.4, 128.8 (C₁₁); 129.0, 129.2 (C₁₂); 129.7 (C₁₃); 131.0 (C₁₄); 132.1, 132.2 (C₁₅); 133.8, 134.0 (C₁₆); 135.4, 135.5 (C₁₇); 136.3, 136.4 (C₁₈); 139.3, 139.5 (C₁₉); 149.2, 149.6 (C₂₀); 155.7, 155.8 (C₂₁). ³¹P-NMR (DMSO-*d*₆, δ , ppm): 28.68, 32.53.

The AP was synthesized following the reported literature.²⁰ In a 250-mL three-necked round-bottomed flask equipped with a magnetic stirrer and a reflux condenser, SB (0.05 mol, 15.81 g) and diethyl phosphite (0.5 mol, 69.02 g) were mixed. After the reaction mixture was stirred at 55 °C for 4 h, the reaction mixture was filtered and washed with ethanol thoroughly. Then, the raw product was recrystallized from DMF/water (1:1) and dried at 70 °C in a vacuum oven for 24 h. The light-yellow solid was collected (15.67 g, yield: 52.9%). FTIR (KBr, cm^{-1}): 3399 (N—H); 3114 (O—H); 2988, 2868 (—CH₃); 2941, 2835 (—CH₂—); 1198 (P=O); 1052, 1022 (P—O—C); 979 (P—O). ¹H-NMR (DMSO-*d*₆, δ , ppm): 0.90–1.02 (6H, —CH₃); 1.12–1.23 (6H, —CH₃); 3.50–4.12 (8H, —CH₂—); 4.92–5.12 (2H, P—C—H); 5.36–5.46 (2H, —NH—); 6.42–7.40 (12H, Ar-H); 9.66–9.72 (2H, —OH). ¹³C-NMR (DMSO-*d*₆, δ , ppm): 16.5, 16.8 (C₁); 47.3, 49.0 (C₂); 62.6, 62.9 (C₃); 114.8 (C₄); 115.2 (C₅); 119.4 (C₆); 123.8 (C₇); 128.7 (C₈); 129.1 (C₉); 139.4 (C₁₀); 155.5 (C₁₁). ³¹P-NMR (DMSO-*d*₆, δ , ppm): 23.95.

Preparation of Epoxy Thermosets

Modified epoxy thermosets were prepared via thermal curing reactions among DGEBA, DDM, and DAP (or AP). In view of the active proton numbers in DAP, AP, and DDM, the formulations of modified epoxy thermosets are listed in Table I, where the sum amount of phenolic and amine protons are equal to the amount of epoxy groups in DGEBA. Briefly, DAP (or AP) and DDM were blended homogeneously at 120 °C for 30 min. When the temperature decreased to 90 °C, the DGEBA was introduced into the mixture and mixed for 10 min. Then, the reaction mixture was transferred into preheated PTFE molds and degassed in a vacuum oven at 100 °C for 5 min. Subsequently, the mixture was cured in a convection oven at 120 °C for 2 h and then postcured at 160 °C for 2 h. Finally, to prevent cracking, the modified thermosets were cooled down slowly to room temperature. The neat epoxy thermoset was also prepared under similar processing condition, but without DAP and AP.

Characterization

All spectra were carried out at room temperature on a Bruker Avance Spectrometer (400 MHz) using DMSO-*d*₆ as solvent and calibrated at 2.50 ppm (¹H) and 39.52 ppm (¹³C).

FTIR spectra were recorded between 400 and 4000 cm^{-1} with a resolution of 4 cm^{-1} on a Varian 640-IR spectrometer (Varian, USA) with KBr pellets.

Elemental analysis of nitrogen was determined by an Elementar Vario EL III elemental analyzer (Elementar Analysensysteme GmbH, Germany) according to the JY/T 017–1996. The phosphorus content was analyzed by an inductively coupled plasma-atomic emission spectrometer (Leeman Prodigy, USA) complying with the JY/T 015–1996.

LOI value was determined using an oxygen index instrument (ATS FAAR, Italy) according to ASTM D-2863-06 with the specimen size of 130 mm × 6.5 mm × 3 mm; The UL-94 vertical test was implemented according to GB/T 2408-2008 with the specimen size of 130 mm × 12.7 mm × 3 mm.

Dynamic mechanical analysis (DMA) was carried out with a DMA Q800 instrument (TA, USA) in the single-cantilever mode from 30 to 230 °C at a heating rate of 10 °C/min, with a frequency of 1 Hz and an amplitude of 15 μm . The specimen dimensions were 35 mm × 6.5 mm × 3 mm.

Thermogravimetric analysis (TGA) was performed by a TG 209 F1 thermal analyzer (NETZSCH, Germany) at a heating rate of

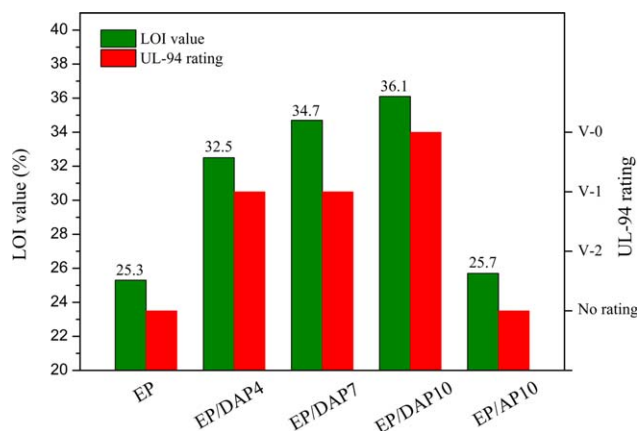


Figure 1. LOI value and UL-94 rating of epoxy thermostets. [Color figure can be viewed in the online issue, which is available at wileyonlinelibrary.com.]

10 °C/min in a temperature range from 30 to 800 °C, under an air or a nitrogen flow of 20 mL/min.

A scanning electron microscope (Hitachi TM-1000, Japan) was used to observe the morphologies of char residues. Samples were sputter-coated with gold before observation.

Laser Raman spectra were recorded with a SPEX-1403 laser Raman spectrometer (SPEX Co., USA) at room temperature with the excitation provided in backscattering geometry by a 633-nm argon laser line. For each char samples, eight different parts were randomly chosen and analyzed.

Py-GC/MS analysis was performed by a system combined with a FRONTIER PY-2020iD Pyrolyser and a SHIMADZU GC-MS QP-2010 Ultra. The sample weight was about 2.0 mg, and the pyrolysis temperature was 600 °C. The carrier gas flow (helium, 1 mL/min) was split in a ratio of 1:30 before being introduced into the gas chromatograph. For the separation, the temperature program of the capillary column (HP DB-5MS, 30 m length, 0.25 mm diameter, and 0.25 μm film thickness) of GC was 3 min at 40 °C and then increased to 300 °C with a heating rate of 15 °C/min and maintained at 300 °C for 10 min.

RESULTS AND DISCUSSION

Flame-Retardant Properties of Epoxy Thermostets

Flame-retardant properties of epoxy thermostets were quantitatively evaluated by LOI and UL-94 test. As shown in Figure 1, neat EP has an LOI value of 25.3%, and it fails in UL-94 test. In contrast, the thermostet modified with DAP shows improved flame retardancy, reflecting in a higher LOI value and rating in UL-94 test. The LOI value raises following the increase of DAP content, and it increases from 32.5% for EP/DAP4 to 34.7% for EP/DAP7. With the incorporation of 10 wt % DAP, the epoxy thermostet achieves an LOI value of 36.1% and V-0 rating in UL-94 test. In the case of EP/AP10, surprisingly, the LOI value is found to be 25.7%, which is close to that of neat EP. Besides, it has no rating in UL-94 test, suggesting that the AP incorporated has no noticeable effect on improving the flame retardancy of epoxy thermostet.

To visibly discern the difference of burning behaviors between neat EP and modified epoxy thermostets, a digital camera was used to record the combustion processes of epoxy thermostets during UL-94 test. The corresponding video screenshots are shown in Figure 2. Apparently, neat EP is ignited quickly with rapid flame propagation, and it burns vigorously with serious flaming drips, which suggests that it is highly combustible. In the case of thermostets modified with DAP, the burning behaviors differ from that of neat EP, and they all extinguish spontaneously. With the increase of DAP content, the burning times after the first and the second applications of the flame decrease gradually. In addition, it is interesting to note that the pyrolytic gases eject from the surface of char layer continuously during combustion, and the burning thermostets seem to be blown out by the ejected pyrolytic gases. This interesting phenomenon, termed the “blowing-out effect” by Zhang *et al.*,²¹ has also been reported in epoxy resin flame retarded by DOPO-POSS during combustion. In regard to EP/AP10, the burning behavior is similar to that of neat EP, whereas the flaming drips are not observed during the test, suggesting that the incorporation of AP slightly improves the flame retardancy of epoxy thermostet.

The photographs of char residues after UL-94 test were also recorded by a digital camera. As presented in Figure 3, neat EP exhibits bits of residual char with a fragmented morphology, even though it is extinguished by artificial factor. As for EP/DAP7 and EP/DAP10, the char residues show intumescent morphologies. Interestingly, some cracked holes (highlighted by the dotted ellipses) resulting from the ejected pyrolytic gases from the char layer are observed on the surface of char residue, complying with the blowing-out phenomenon observed during combustion. With respect to EP/AP10, surprisingly, it displays a loose char layer, and there are some tiny holes on the surface of residual char. Such a char layer is not sufficient to provide good insulation to the underlying matrix from the heat, thus resulting in inferior flame retardancy. The micromorphologies of char layers for thermostets corresponding to the blue box in Figure 3, and the deep reason behind the difference of flame-retardant properties between epoxy thermostet modified with AP and DAP, respectively, will be explored in the following section.

Dynamic Mechanical Properties of Epoxy Thermostets

Figure 4 presents DMA plots of the storage modulus and loss factor $\tan \delta$ as a function of temperature for epoxy thermostets, and the corresponding data such as glass transition temperature (T_g) and crosslinking density (ν_e) are summarized in Table II. The value of T_g is obtained from the peak temperature of $\tan \delta$. The ν_e values for thermostets can be determined using the theory of rubber elasticity and calculated according to the following equation^{22–24}:

$$E' = 3\nu_e RT, \quad (1)$$

where E' denotes the storage modulus of the thermostet at $T_g + 50$ °C in the rubbery plateau region, R is the gas constant, and T is the absolute temperature at $T_g + 50$ °C.

As shown in Table II, the value of ν_e reduces with the increase of DAP content in epoxy thermostet. It is possible that the steric hindrance effect, induced by the bulky and rigid DOPO unit in

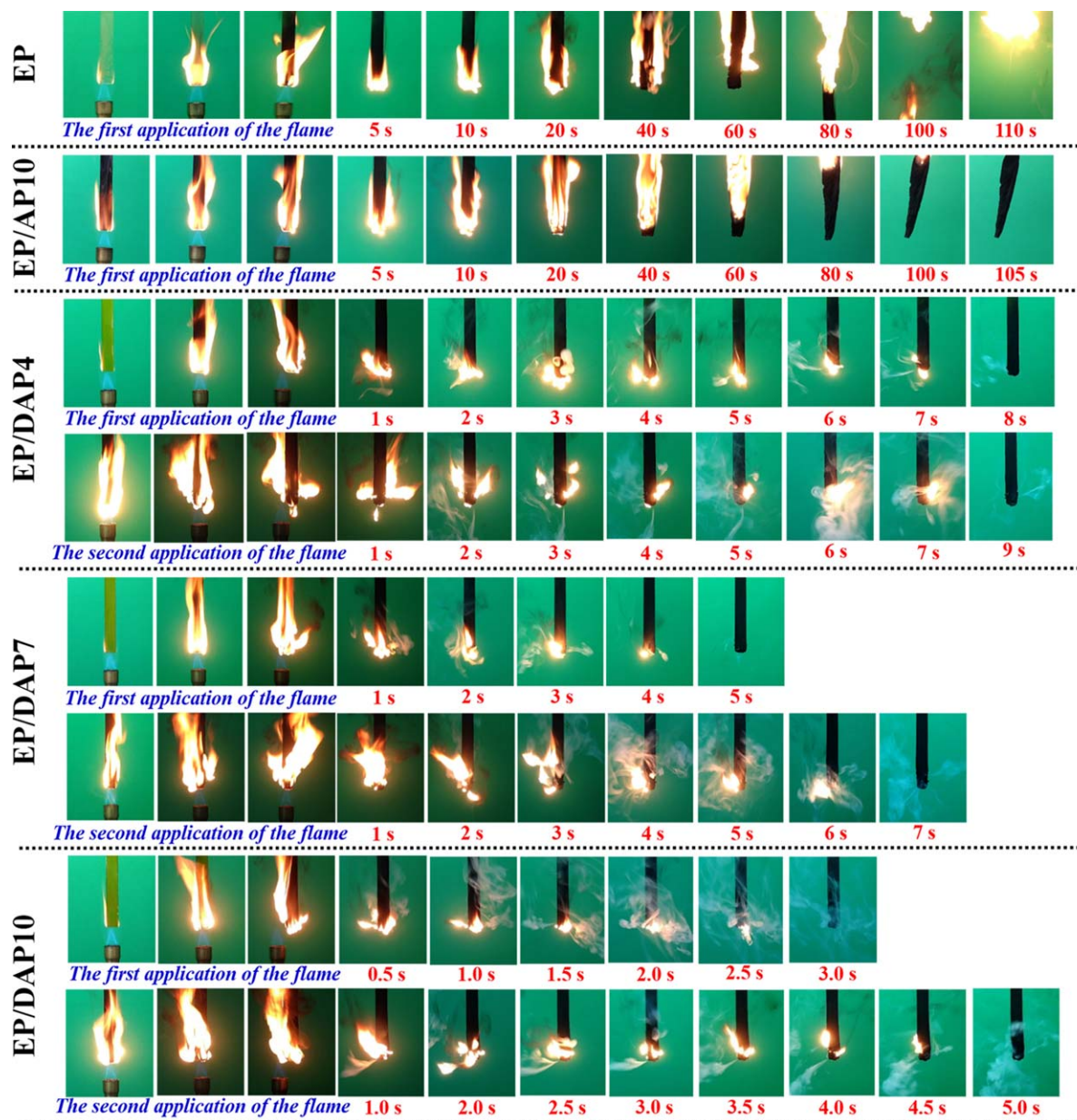


Figure 2. Video screenshots of epoxy thermostets during UL-94 test. [Color figure can be viewed in the online issue, which is available at wileyonlinelibrary.com.]

DAP moiety, may raise the activation energy of the curing reaction between epoxy resin and curing agent, thus resulting in the reduction of crosslinking density for thermostet.²⁵ In terms of

the value of T_g , it decreases from 171.8°C for EP to 162.1°C for EP/DAP4 and to 151.4°C for EP/DAP10. It should be noted that the value of T_g for EP/API10 is lower than those of EP/

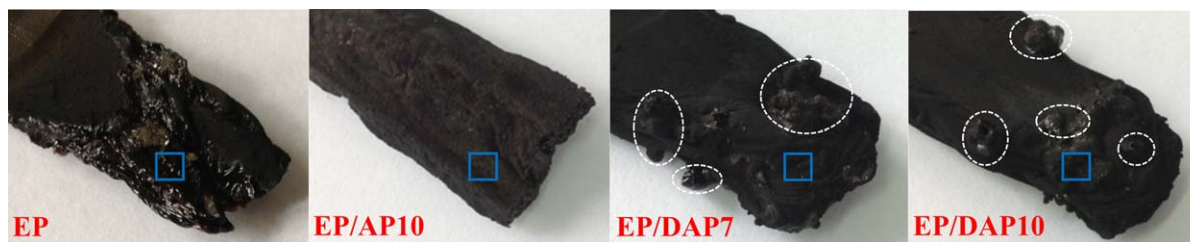


Figure 3. Digital photos of char residues for epoxy thermostets after UL-94 test. [Color figure can be viewed in the online issue, which is available at wileyonlinelibrary.com.]

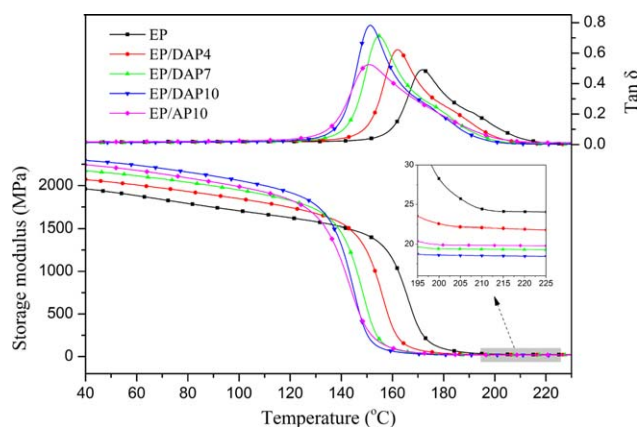


Figure 4. DMA curves of epoxy thermosets. [Color figure can be viewed in the online issue, which is available at wileyonlinelibrary.com.]

DAP7 and EP/DAP10, although the crosslinking density of EP/AP10 is higher. In view of the fact that apart from the crosslinking density, the value of T_g for epoxy networks is also dependent on the chemical structure of the chain segment.²⁴ The bulky and rigid DOPO unit in DAP moiety may restrain the mobility of macromolecular chains, thus compensating for the decrease of crosslinking density. In contrast, the flexible ethoxy group in AP moiety reduces the rigidity of macromolecular chains, which possibly leads to the reduction of T_g .²⁶

Thermal Stabilities of DAP, AP, and Epoxy Thermosets

To investigate the effect of DAP and AP incorporated on the thermal stabilities of epoxy thermosets, TGA was carried out under nitrogen atmosphere, as well as in air. The TGA curves of DAP, AP, and epoxy thermosets are depicted in Figure 5, and the corresponding data such as the 5 wt % mass loss temperature ($T_{5\%}$), the maximum mass loss rate (V_{\max}), the temperature at V_{\max} (T_{\max}), and the char yield at 600 °C are summarized in Table III.

Under nitrogen atmosphere, the AP begins to degrade at around 180 °C and undergoes a 34 wt % weight loss in the temperature range of 180–210 °C. For DAP, the initial degradation temperature is found to be at about 240 °C, which is higher than that of AP. This can be ascribed to the fact that the cyclic O=P—O chain protected by phenylene group is more thermally stable than the open O=P—O chain.^{27,28} In regard to epoxy thermosets, they all display a single decomposition process, corresponding to the thermal degradation of molecular chains. As shown in Table III, in comparison with neat EP, the incorporation of DAP results in a lower $T_{5\%}$ for modified thermoset, and it decreases from 354.9 °C for neat EP to 301.4 °C for EP/DAP10. Besides, the value of $T_{5\%}$ for thermoset decreases following the increase of DAP content. To explain this phenomenon, it should be noted that the O=P—O bond in DAP moiety is less stable than the common C—C bond,^{29,30} and moreover, the introduction of DAP decreases the crosslinking density of epoxy thermoset as discussed above. These two factors possibly account for a lower value of $T_{5\%}$ for thermoset modified with DAP. With respect to EP/AP10, the value of $T_{5\%}$ (271.7 °C) is lower than that of EP/DAP10, which is due to the lower thermostability of open O=P—O chain in AP moiety as

mentioned above. Furthermore, it can be observed that all the modified thermosets possess higher char yields at elevated temperatures when compared with neat EP, suggesting that the introduction of both DAP and AP into thermosets can promote the formation of char residues.

In the case of air atmosphere, it is clear that the presence of oxygen complicates the decomposition process for all the epoxy thermosets, and one additional weight loss is observed at elevated temperatures, which is ascribed to the further oxidation decomposition of char residues. Similar to the results obtained in nitrogen, both DAP and AP incorporated into thermosets result in the reduction of $T_{5\%}$, and the increase of char yield at 600 °C. For example, the char yield at 600 °C increases sharply from 7.9% for neat EP to 13.0% for EP/DAP10 and to 18.6% for EP/AP10. It is possible that phosphorus-based acid such as phosphoric acid and polyphosphoric acid, generated from the thermal degradation of DAP and AP moiety in thermosets, can react with the decomposed matrix to promote the formation of char residues.^{31,32}

It is worth noting that EP/AP10 possesses a higher char yield than EP/DAP10 at elevated temperature in both air and nitrogen, whereas it achieves inferior flame retardancy as mentioned previously. In view of the loose char layer of EP/AP10 presented in Figure 3, it is not difficult to speculate that the quality rather than the amount of residual char plays a pivotal role in enhancing the flame retardancy of epoxy thermoset.

Thermo-Oxidative Degradation Behaviors of DAP, AP, and Epoxy Thermosets

To gain insight into the flame-retardant mechanism of modified epoxy thermosets in the condensed phase, the FTIR spectra at different temperatures were used to investigate the thermo-oxidative degradation behaviors of DAP, AP, neat EP, EP/DAP10, and EP/AP10. Samples were treated in muffle furnace at a heating rate of 10 °C/min under air atmosphere. The solid residues were gathered when heated to specified temperature and characterized by FTIR.

Figure 6 shows the FTIR spectra of DAP and AP at different temperatures. As to DAP, several peaks including 1594, 1475 cm^{-1} (P—C_{Ar}), 1215 cm^{-1} (P=O), and 1195, 934 cm^{-1} (P—O—C_{Ar}) are observed in the spectrum at 25 °C, which are attributed to the absorptions of DOPO group. The spectrum at 250 °C is nearly the same as that at 25 °C, confirming that DAP is thermally stable below 250 °C, which has been suggested by TGA results. At 300 °C, the relative intensities of absorption peaks attributed to DOPO group decrease, implying that DOPO

Table II. T_g and Crosslinking Density Values for Epoxy Thermosets

Sample	E' (MPa)	T_g (°C)	v_e (mol/m ³)
EP	24.1	171.8	1952
EP/DAP4	22.0	162.1	1818
EP/DAP7	19.4	154.8	1627
EP/DAP10	17.6	151.4	1487
EP/AP10	19.9	150.9	1683

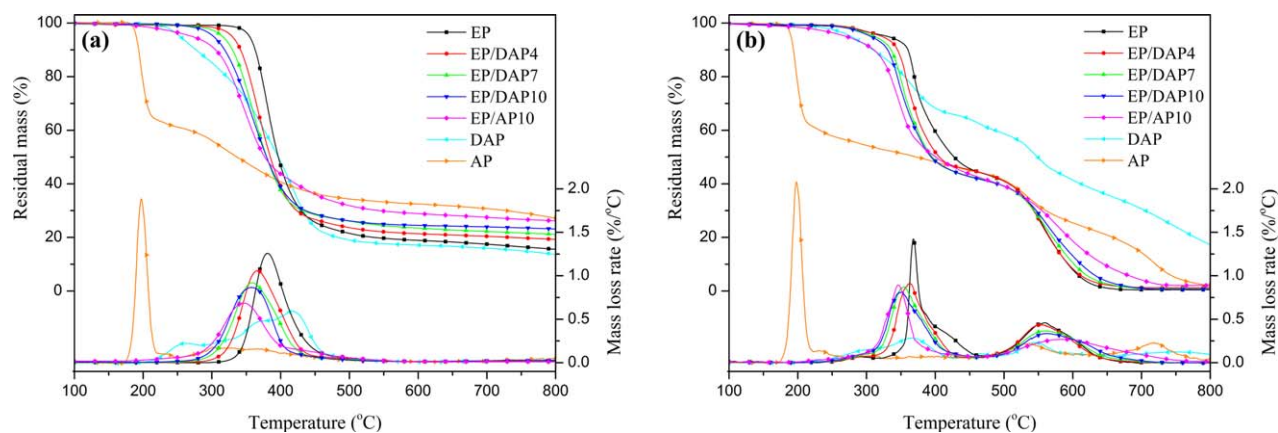


Figure 5. TGA curves of DAP, AP, and epoxy thermostets in nitrogen (a) and air (b). [Color figure can be viewed in the online issue, which is available at wileyonlinelibrary.com.]

Table III. TGA Data of Epoxy Thermostets in Nitrogen and Air

Sample	$T_{5\%}$ (°C)		T_{max} (°C)		V_{max} (%/°C)		Char yield at 600 °C (%)	
	N ₂	Air	N ₂	Air	N ₂	Air	N ₂	Air
EP	354.9	331.1	380.9	368.1, 558.6	1.29	1.43, 0.46	18.9	7.9
EP/DAP4	330.1	322.4	366.3	362.9, 554.9	1.07	0.91, 0.43	21.4	8.3
EP/DAP7	314.2	311.5	359.4	353.5, 559.9	0.91	0.87, 0.36	23.6	10.6
EP/DAP10	301.4	306.4	357.3	351.4, 561.4	0.86	0.81, 0.33	24.5	13.0
EP/AP10	271.7	270.5	346.1	345.7, 588.2	0.69	0.89, 0.27	28.9	18.6

moiety in DAP is partly released to the gas phase. Meanwhile, some new peaks at 1616, 1237, 1155, 1094, 1054, and 532 cm^{-1} are detected in the spectrum, which are assigned to the characteristic absorptions of O=P—OH group, suggesting the formation of phosphoric acid.^{33–35} When the temperature increases to 450 °C, new peaks at 905 and 501 cm^{-1} due to the stretching vibration of P—O—P bond and the bending vibration of

O—P—O bond, respectively, appear, indicating that polyphosphoric acid is formed by the dehydration of P—OH bond.^{33,36}

In the case of AP, the absorptions at 3000 to 2800 cm^{-1} in the spectrum at 25 °C are assigned to the stretching vibrations of —CH₃ and —CH₂— groups, and several peaks at 1198 cm^{-1} (P=O), 1052, 1022 cm^{-1} (P—O—C), and 979 cm^{-1} (P—O) are also identified. At 300 °C, it is obvious that the absorptions due to

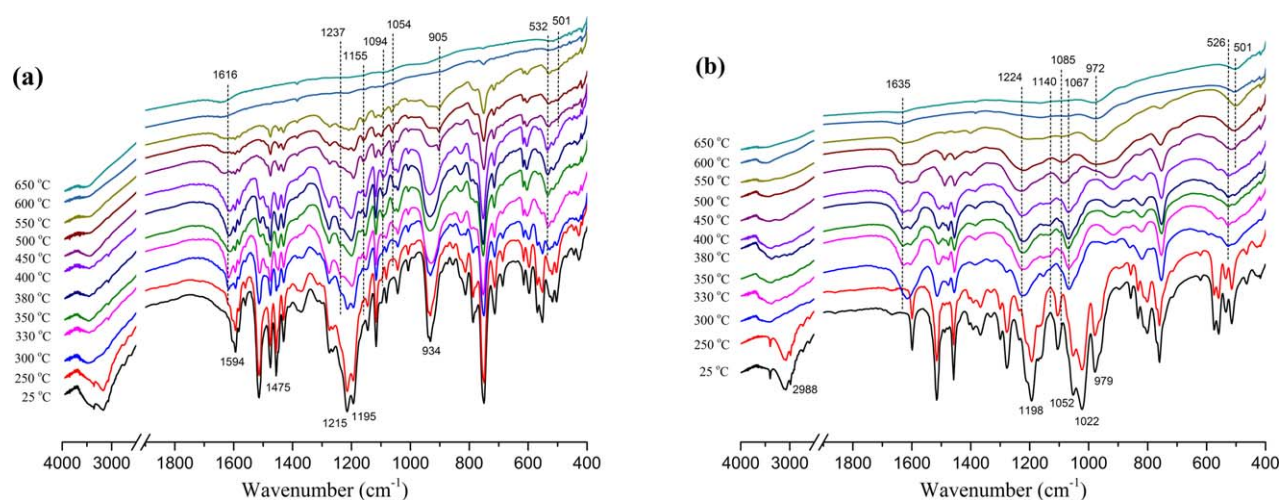


Figure 6. FTIR spectra of DAP (a) and AP (b) at different temperatures. [Color figure can be viewed in the online issue, which is available at wileyonlinelibrary.com.]

the stretching vibrations of $-\text{CH}_3$ and $-\text{CH}_2-$ groups vanish, and the peaks at 1052 and 1022 cm^{-1} ascribed to absorptions of $\text{P}-\text{O}-\text{C}$ bond disappear thoroughly, which means that the break of $\text{P}-\text{O}-\text{ethyl}$ bond and the disappearance of $-\text{OCH}_2\text{CH}_3$ group.^{35,37} This can be regarded as an indirect sign that ethanol is generated and released into the gas phase during the early degradation of AP. In the meantime, new absorption peaks at 1635 , 1224 , 1140 , 1085 , 1067 , and 526 cm^{-1} due to the characteristic absorptions of $\text{O}=\text{P}-\text{OH}$ group are detected, which indicates the formation of phosphoric acid. As the temperature increases to 450°C , similar to the spectrum of DAP at 450°C , new peaks at 972 and 501 cm^{-1} assigned to the stretching vibration of $\text{P}-\text{O}-\text{P}$ bond and the bending vibration of $\text{O}-\text{P}-\text{O}$ bond appear in the spectrum, suggesting the formation of polyphosphoric acid. Based on the analysis above, it can be stated that phosphoric acid can be formed during the early thermo-oxidative degradation of both DAP and AP and then converted to polyphosphoric acid due to the further thermal decomposition.

Figure 7 shows the FTIR spectra of neat EP, EP/DAP10, and EP/AP10 at different temperatures. For neat EP, the typical absorptions are observed at 3438 , 2965 , 2871 , 1609 , 1509 , 1460 , 1362 , 1245 , 1182 , 1036 , and 828 cm^{-1} at 25°C .^{1,38} It is obvious that the relative intensities of typical absorption peaks decrease drastically when the temperature is above 330°C , and the characteristic peaks disappear completely at 500°C , implying that the main degradation of neat EP occurs in this temperature range, which is consistent with the results obtained from TGA. At 350°C , two additional peaks at 1726 and 1657 cm^{-1} are detected in the spectrum, which are assigned to the absorptions of carbonyl group and amide group, respectively. The formation of carbonyl group arises from the oxidation of the secondary alcohol groups in epoxy thermoset,³⁹ whereas that of amide group originates from oxidation of the α -amino carbon belonging to the chain segments.⁴⁰ As the temperature exceeds 500°C , the typical absorption peaks at 1609 , 1509 , and 1460 cm^{-1} due to $\text{C}=\text{C}$ stretching vibration in aromatic ring vanish, whereas a new broader peak at 1594 cm^{-1} shows up, manifesting the formation of polyaromatic structures.^{41,42}

In the case of EP/DAP10 and EP/AP10, it can be found that in the range of 25 to 500°C , the spectra are similar to those of neat EP. The only noticeable difference is the additional peak at 756 cm^{-1} , which is attributed to the $\text{C}_{\text{Ar}}-\text{H}$ deformation vibration from the ortho-substituted aromatic ring in DAP and AP moiety. Other absorption bands originating from the DAP and AP moiety are concealed by strong absorptions of the epoxy matrix. When the temperature is above 500°C , several new absorption peaks are detected in the spectra of residual chars for EP/DAP10 and EP/AP10, apart from the peak at 1594 cm^{-1} due to the absorption of polyaromatic structures. As to EP/DAP10, the peak at 1096 cm^{-1} belongs to the stretching vibration of $\text{P}-\text{O}-\text{C}_{\text{Ar}}$ bond,^{35,43} and peaks at 983 and 500 cm^{-1} are attributed to the stretching vibration of $\text{P}-\text{O}-\text{P}$ bond and the bending vibration of $\text{O}-\text{P}-\text{O}$ bond, respectively.⁴⁴ For EP/AP10, the absorptions at 1092 , 980 , and 510 cm^{-1} assigned to $\text{P}-\text{O}-\text{C}_{\text{Ar}}$, $\text{P}-\text{O}-\text{P}$, and $\text{O}-\text{P}-\text{O}$ bonds, respectively, are also observed in the spectrum. With the fact that phosphoric acid and polyphosphoric acid can be formed during the thermo-

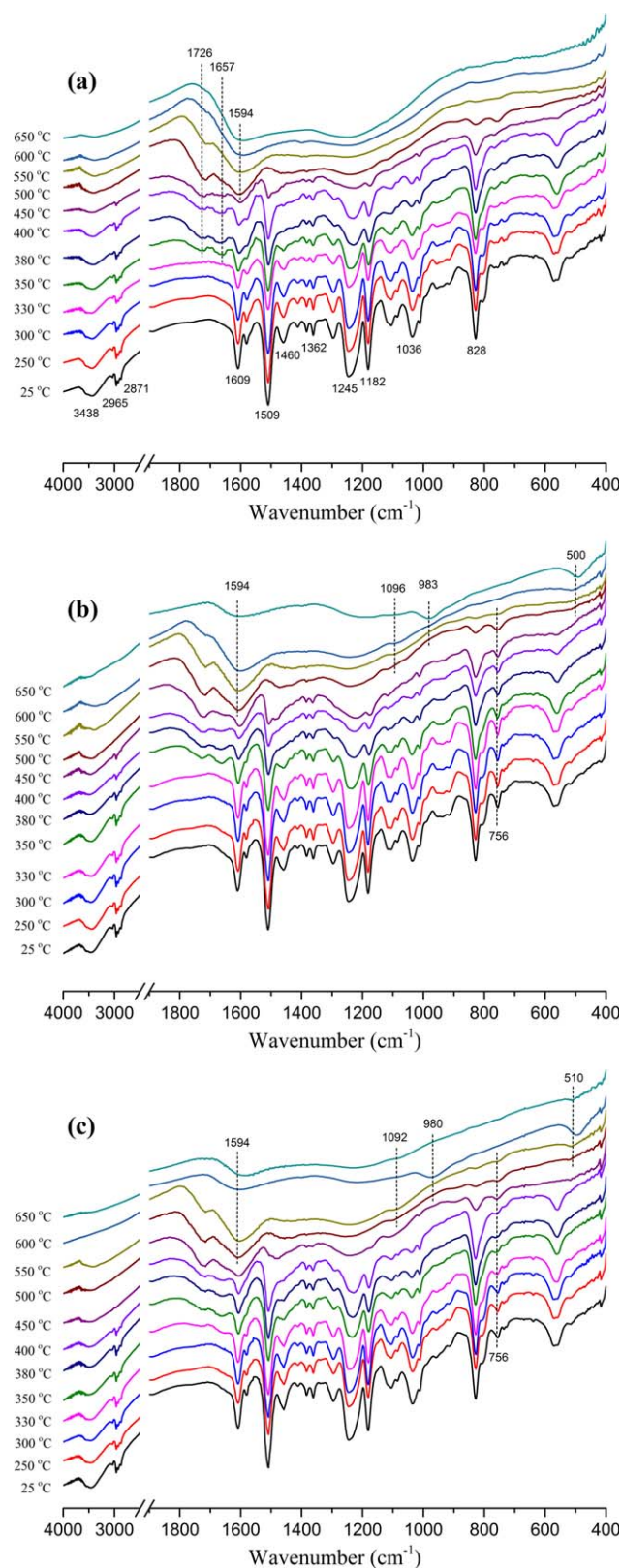


Figure 7. FTIR spectra of neat EP (a), EP/DAP10 (b), and EP/AP10 (c) at different temperatures. [Color figure can be viewed in the online issue, which is available at wileyonlinelibrary.com.]

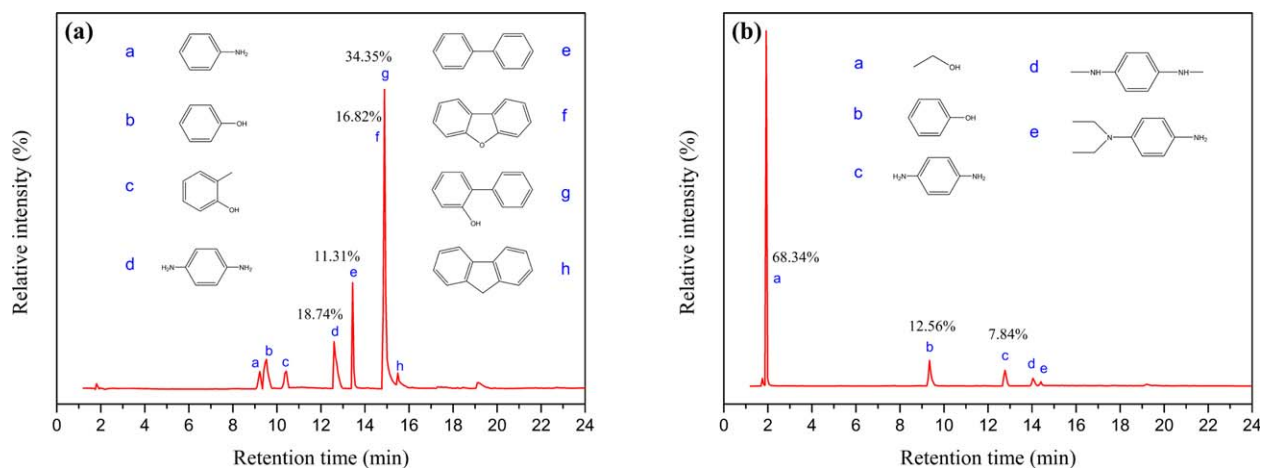


Figure 8. Pyrograms and assigned products of DAP (a) and AP (b). [Color figure can be viewed in the online issue, which is available at wileyonlinelibrary.com.]

oxidative degradation of both DAP and AP as demonstrated above, it is reasonable to state that the acids can esterify and dehydrate the decomposed epoxy matrix to promote the formation of phosphorus-rich char layers with polyaromatic structures bridged by P—O—C and P—O—P bonds.

Pyrolysis Behaviors of DAP, AP, and Epoxy Thermosets

It is generally accepted that phosphorus-based flame retardant not only plays flame-retardant role in the condensed phase but also in the gas phase. To understand the flame-retardant mechanism of modified epoxy thermosets in the gas phase, the Py-GC/MS was used to analyze the pyrolysis products of DAP, AP, neat EP, EP/DAP10, and EP/AP10.

Figure 8 shows the pyrograms and corresponding pyrolytic products of DAP and AP. It is clear that the main pyrolytic products of DAP are *p*-phenylenediamine, diphenyl, dibenzofuran, and *o*-phenylphenol, the relative areas of which are 18.74%, 11.31%, 16.82%, and 34.35%, respectively. The formation of dibenzofuran is ascribed to the splitting of P—C and P—O bonds of DOPO-based derivative, which can be considered as a sign for the existence of phosphorus-based fragments in the gas phase.^{45,46} For AP, the main pyrolytic products are ethanol, phenol, and *p*-phenylenediamine, the relative areas of which are 68.34%, 12.56%, and 7.84%, respectively. In consideration of the result obtained from the investigation of thermo-oxidative degradation behavior for AP, it can be confirmed that the early degradation of AP produces massive and highly combustible ethanol.

Figure 9 shows the pyrograms of EP, EP/DAP10, and EP/AP10, and the pyrolytic products identified in the pyrograms of EP/DAP10 and EP/AP10 are summarized in Table IV. The main pyrolysis products of EP are phenol (94 *m/z*), 4-isopropylphenol (136 *m/z*), 4-isopropenylphenol (134 *m/z*), 4-(2-phenylpropan-2-yl) phenol (212 *m/z*), and 2-methyl-4-(2-phenylpropan-2-yl) phenol (226 *m/z*). It can be clearly seen that after the incorporation of DAP or AP into epoxy thermoset, the types of pyrolytic products are altered.

In terms of EP/DAP10, it is worth noting that some pyrolytic products originating from the pyrolysis of DAP moiety, including diphenyl, dibenzofuran, and *o*-phenylphenol, are detected, implying that phosphorus-based fragments are released into the gas phase during pyrolysis as discussed above. The phosphorus-based fragments such as PO and PO₂ free radicals can capture the H and OH free radicals in the flame and exert quenching effect on the free radical chain reaction of combustion. Furthermore, it can be found that there are considerable CO₂ and nitrogen-based compounds in the pyrolytic products of EP/DAP10. The nitrogen-based compounds may be converted to nonflammable gases such as N₂, NH₃, and NO₂ during combustion,^{8,47} which can work jointly with CO₂ to dilute ignitable gases, cut off the supply of oxygen, and take away the heat produced during combustion.⁸ In summary, the flame-retardant mechanism of EP/DAP10 in the gas phase is attributed to the quenching effect of phosphorus-based free radicals and diluting effect of nonflammable gases.

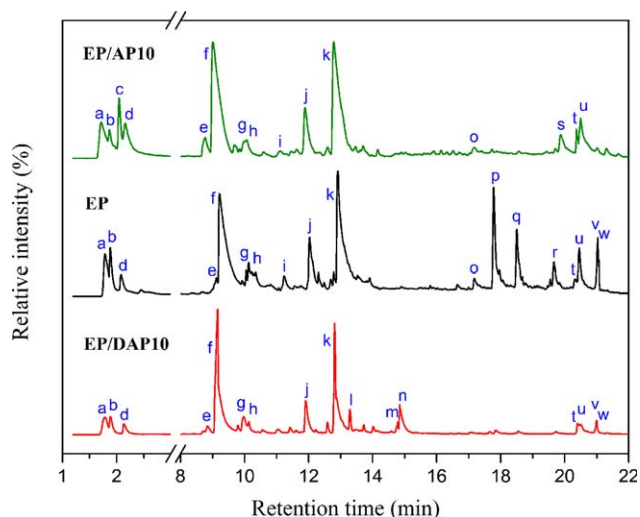
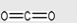






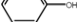







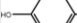


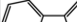
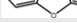
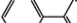




Figure 9. Pyrograms of EP, EP/DAP10, and EP/AP10. [Color figure can be viewed in the online issue, which is available at wileyonlinelibrary.com.]

Table IV. Pyrolytic Products Identified in the Pyrograms of EP/DAP10 and EP/AP10

No.	m/z	Assigned structure	Relative area (%)	
			EP/DAP10	EP/AP10
a	44		3.3	4.2
b	44		2.3	2.8
c	46		—	5.6
d	58		1.3	3.7
e	118		1.5	2.3
f	94		33.2	31.2
g	120		4.1	1.4
h	132		1.5	1.6
i	134		<1	1.4
j	136		6.6	7.4
k	134		22.2	26.7
l	154		2.7	—
m	168		2.6	—
n	170		6.7	—
o	183		<1	1.2
p	212		<1	<1
q	226		<1	<1
r	242		<1	<1
s	198		—	3.4
t	228		1.5	2.4
u	252		2.7	3.9
v	240		1.1	<1
w	254		1.6	<1

In the case of EP/AP10, nitrogen-based compounds are also observed during pyrolysis. These compounds may be transformed into nonflammable gases during combustion, thus exerting flame-retardant effect in the gas phase. However, it should be noted that ethanol with a high relative area of 5.6% is detected in the pyrolytic products, which is generated from

the pyrolysis of AP moiety in EP/AP10 as mentioned previously. Moreover, the relative areas of other highly combustible gases such as aldehyde and acetone are also higher than that of EP/DAP10. These results reveal that EP/AP10 produces more highly combustible gases when compared with EP/DAP10 during pyrolysis, which can provide adequate fuels to accelerate the combustion process.

Morphology and Structure of Residual Char

It is already known that flame retardancy is related to char morphology and architecture, and a compact and integrated char layer on the surface of matrix can block the release of gaseous fuel and prevent the transfer of heat back to the burning polymer. To further disclose the flame-retardant mechanism in the condensed phase, the micromorphologies of char layers corresponding to the blue box in Figure 3 for epoxy thermosets after UL-94 test were investigated by SEM as shown in Figure 10.

The exterior char layer of neat EP presents obvious cracks, and the interior char layer displays disconnected feature, which can be ascribed to the pyrolytic gases breaking through the incomplete char layer during combustion. In terms of EP/AP10, the morphologies of exterior and interior char layer are similar to those of neat EP. It is possible that the early degradation of AP moiety in EP/AP10 produces a large amount of combustible gases especially ethanol as mentioned above, which can provide adequate fuels to accelerate the combustion process, thus leading to the release of massive pyrolytic gases. Meanwhile, the charring process does not proceed sufficiently, and the pre-formed char layer is not compact enough to block gases breaking through, which results in the formation of a loose char layer. In the case of EP/DAP7 and EP/DAP10, the intumescent and compact char layers are observed on the surface. Moreover, the interior char layers show honeycombed structure with considerable holes running through. This intumescent and compact char layer with honeycombed cavity inside can not only serve as a superior barrier to isolate the oxygen and heat from the underlying matrix but also accumulate pyrolytic gases containing phosphorus-based free radicals and nonflammable gases during combustion. The flame is blown out by the intensively released gases when the amount of pyrolytic gases goes beyond the holding capacity of the char layer, thus appearing the blowing-out effect.

The graphitization degree of residual char is a very important structural parameter, which reflects the transition extent of carbon material from turbostratic to graphitic structure.⁴⁸ The residual char with a higher graphitization degree is more conducive in suppressing the diffusion of heat and mass during pyrolysis owing to its higher thermal stability and compactness.⁴⁹

Laser Raman spectroscopy was used to investigate the graphitic structure of char residues. Samples were thermally treated from room temperature to 600 °C with a heating rate of 10 °C/min under air atmosphere in muffle furnace. Then, the residues were gathered and analyzed by laser Raman spectroscopy. As shown in Figure 11, all the spectra display two peaks at 1360 cm⁻¹ (D band) and 1593 cm⁻¹ (G band), which are assigned to the vibration of the carbon atoms in disordered graphite or glassy carbons and the carbon atoms in crystalline graphite,

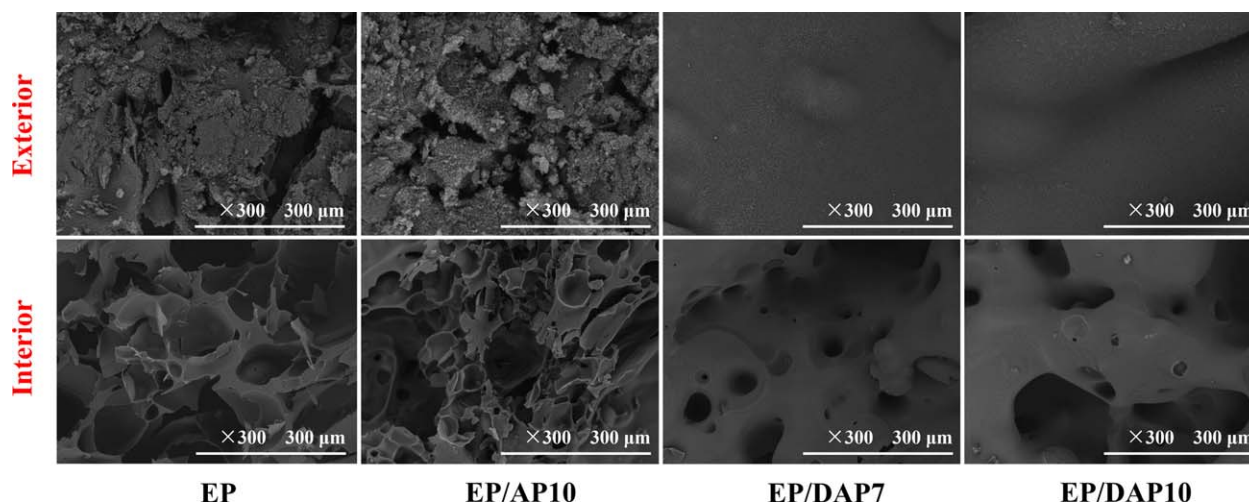


Figure 10. SEM micrographs of char residues for epoxy thermostets after UL-94 test. [Color figure can be viewed in the online issue, which is available at wileyonlinelibrary.com.]

respectively. In general, the ratio of the integrated intensity of D and G bands (I_D/I_G) is inversely proportional to the graphitization degree of the residual char, and a lower I_D/I_G value means a higher graphitization degree of the resultant char.^{48,50} The I_D/I_G value reported here for each resultant char was the average of eight measurements. As presented in Figure 11, the I_D/I_G value of resultant char for thermostet modified with DAP is lower when compared with that of neat EP. This suggests that DAP incorporated endows the resultant char with a higher graphitization degree, which can provide better insulation to the matrix beneath from the heat and oxygen, thus imparting improved flame retardancy to the thermostet. Additionally, it should be noted that the residual char for EP/AP10 has a higher I_D/I_G value than that for EP/DAP10. This indicates that when

compared with EP/DAP10, the char layer of EP/AP10 is not compact and thermally stable enough to inhibit the combustion process, which is in agreement with the result obtained from SEM observation.

To better elucidate the flame-retardant role of phosphorus and nitrogen element in EP/DAP10 and EP/AP10, their contents in thermostets at 25 and 600 °C in air left after TGA were analyzed, and the results are given in Table V. The element loss rate (ELR) introduced herein is defined as the amount of element volatilized into the air during thermal degradation in the range of 25–600 °C, which can be calculated according to the following equation:

$$\text{ELR} = (1 - R_t \times \text{CY}/R_0) \times 100\%, \quad (2)$$

where R_0 and R_t represent the element contents in thermostets at 25 and 600 °C, respectively. CY is the char yield at 600 °C, which has been listed in Table III.

As shown in Table V, the ELR of nitrogen element in EP/DAP10 is 77.69%, which is higher than that in EP/AP10 (64.91%). It reveals that more nitrogen element in EP/DAP10 is released to the gas phase when compared with that in EP/AP10 during thermal degradation, which can promote the flame-retardant effect in the gas phase by diluting combustible gases and oxygen. Besides, the ELR of phosphorus element in EP/DAP10 is 77.27%, which means that the majority of phosphorus element

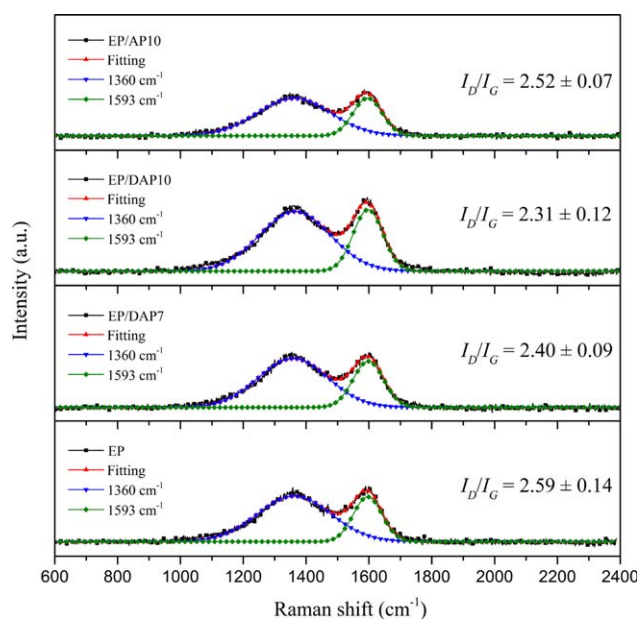


Figure 11. Typical Raman spectra of char residues for epoxy thermostets. [Color figure can be viewed in the online issue, which is available at wileyonlinelibrary.com.]

Table V. Element Contents and Loss Rates for EP/DAP10 and EP/AP10

Sample	Element	Element content (%)		Element loss rate (%)
		25 °C	600 °C	
EP/DAP10	N	2.34	4.02	77.69
	P	0.83	1.44	77.27
EP/AP10	N	2.36	4.46	64.91
	P	1.05	2.41	57.06

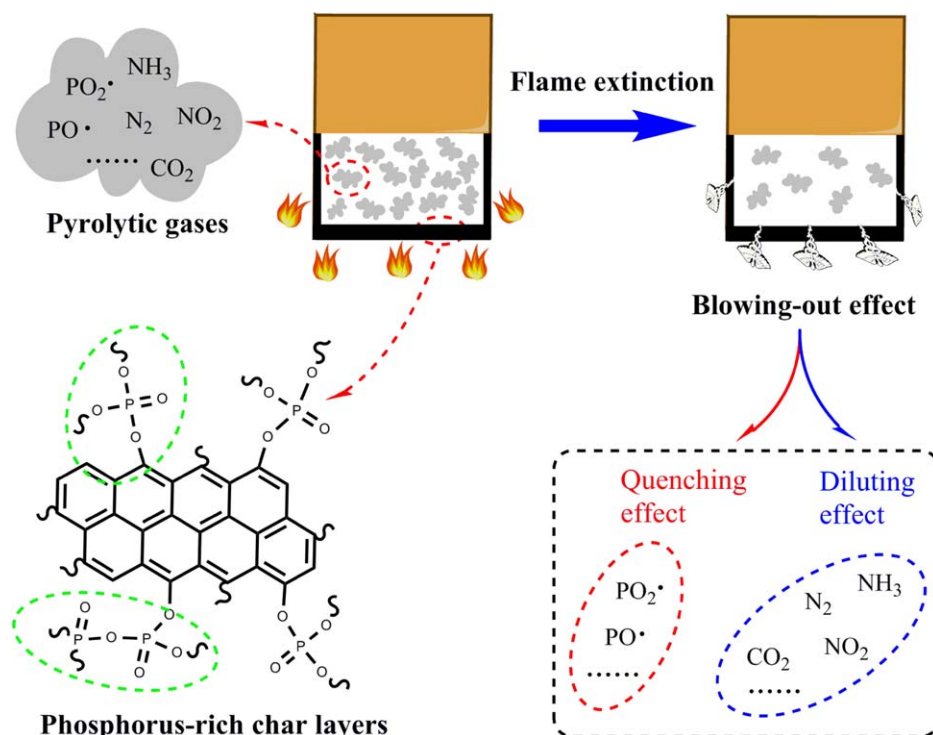


Figure 12. Schematic illustration of blowing-out effect. [Color figure can be viewed in the online issue, which is available at wileyonlinelibrary.com.]

is released to the gas phase. This suggests that DAP incorporated plays flame-retardant role mainly in the gas phase by scavenging the H and OH radicals in the flame. However, the remaining phosphorus element in the condensed phase also plays a pivotal role in the formation of compact and phosphorus-rich char layer with honeycombed cavity inside, which is essential to the appearance of the blowing-out effect during combustion.

It should be noted that the ELR of phosphorus element in EP/AP10 is found to be 57.06%, which is lower than that in EP/DAP10. This means that when compared with EP/DAP10, more phosphorus element in EP/AP10 is reserved in the condensed phase. In view of the fact that phosphorus element in the condensed phase can promote the formation of char residues, it is not difficult to explain the result obtained from TGA that the char yield of EP/AP10 at elevated temperature is higher than that of EP/DAP10.

Flame-Retardant Mechanism

Based on all the above discussions, the flame-retardant mechanism of epoxy thermoset modified with DAP can be elucidated as follows.

In the gas phase, the pyrolysis of thermoset modified with DAP releases considerable phosphorus-based free radicals and nitrogen-based compounds. The phosphorus-based free radicals can capture the H and OH radicals in the flame and exert quenching effect on the free radical chain reaction of combustion. Besides, the nitrogen-based compounds can be converted to nonflammable gases such as N_2 , NH_3 , and NO_2 during combustion, which can cooperate with CO_2 to dilute ignitable gases,

cut off the supply of oxygen, and take away the heat produced during combustion.

In the condensed phase, although the majority of phosphorus element is released to the gas phase, the remaining phosphorus element can be transformed into phosphoric acid and polyphosphoric acid during combustion, which can esterify and dehydrate the decomposed epoxy matrix to promote the formation of phosphorus-rich char layers. The char layers can provide a thermally insulating barrier on the surface of matrix and reduce heat and oxygen transmission into the material.

The blowing-out effect observed during combustion can be briefly illustrated in Figure 12. The phosphorus-based acid, originating from the degradation of DAP moiety in the thermoset, induces the epoxy matrix to form a compact and phosphorus-rich char layer with honeycombed cavity inside on the surface of burning matrix during combustion. This char layer can accumulate pyrolytic gases containing phosphorus-based free radicals such as PO and PO_2 radicals and nonflammable gases like N_2 , NH_3 , NO_2 , and CO_2 . The amount of pyrolytic gases in the char layer increases with the progression of combustion. The flame is blown out by the intensively released gases when the amount of pyrolytic gases exceeds the holding capacity of the char layer, thus showing the blowing-out effect.

In the case of epoxy thermoset modified with AP, although the AP incorporated promotes the formation of phosphorus-rich char layer in the condensed phase and releases nonflammable gases in the gas phase, the mismatching of charring process with the gas emission process during combustion possibly results in inferior flame retardancy. Specifically, the early

degradation of epoxy thermoset modified with AP produces massive and highly combustible gases especially ethanol, which can provide adequate fuels to accelerate the combustion process, thus sparking off the release of a large amount of pyrolytic gases. In the meantime, the charring process does not proceed sufficiently, and the preformed char layer is not compact enough to block such considerable gases breaking through, leading to the formation of a loose char layer with tiny holes. The char layer cannot provide good insulation to the underlying matrix from the heat and restrain combustion process, thus resulting in inferior flame retardancy.

CONCLUSIONS

In this work, two phosphorus-containing phenolic amines (DAP and its analog AP) were used to improve the flame retardancy of epoxy resins. With the introduction of 10 wt % DAP, the epoxy thermoset showed an LOI value of 36.1% and V-0 rating in UL-94 test, whereas the thermoset modified with 10 wt % AP only achieved an LOI value of 25.7% and no rating in UL-94 test. In the case of thermosets modified with DAP, they all showed blowing-out effects during UL-94 test, which were attributed to the intensive release of pyrolytic gases containing phosphorus-based free radicals and nonflammable gases. The flame-retardant mechanism was ascribed to the quenching and diluting effect in the gas phase and the formation of phosphorus-rich char layers in the condensed phase. Although the majority of phosphorus element in the thermoset was released to the gas phase to exert flame-retardant effect, the remaining phosphorus element promoted the formation of compact and phosphorus-rich char layer with cavity inside, which was essential to the appearance of blowing-out effect during combustion. Moreover, the inferior flame retardancy of thermoset modified with AP was possibly assigned to the mismatching of charring process with gas emission process during combustion.

ACKNOWLEDGMENTS

This work was financially supported by the Program for Specialized Research Fund for the Doctoral Program of Higher Education in China (Grant No. 20130075130002) and the National Natural Science Foundation of China (Grant Nos. 51203018 and 51303022).

REFERENCES

1. Zhang, W. C.; Li, X. M.; Yang, R. J. *J. Appl. Polym. Sci.* **2013**, *130*, 4119.
2. Chruściel, J. J.; Leśniak, E. *Prog. Polym. Sci.* **2015**, *41*, 67.
3. Gu, H. B.; Guo, J.; He, Q. L.; Tadakamalla, S.; Zhang, X.; Yan, X. R.; Huang, Y. D.; Colorado, H. A.; Wei, S. Y.; Guo, Z. H. *Ind. Eng. Chem. Res.* **2013**, *52*, 7718.
4. You, G. Y.; Cheng, Z. Q.; Peng, H.; He, H. W. *J. Appl. Polym. Sci.* **2014**, *131*, DOI: 10.1002/app.41079.
5. Gao, M.; Wu, W. H.; Xu, Z. Q. *J. Appl. Polym. Sci.* **2013**, *127*, 1842.
6. Xiong, Y. Q.; Jiang, Z. J.; Xie, Y. Y.; Zhang, X. Y.; Xu, W. J. *J. Appl. Polym. Sci.* **2013**, *127*, 4352.
7. Xu, W. H.; Wirasaputra, A.; Liu, S. M.; Yuan, Y. C.; Zhao, J. Q. *Polym. Degrad. Stabil.* **2015**, *122*, 44.
8. You, G. Y.; Cheng, Z. Q.; Peng, H.; He, H. W. *J. Appl. Polym. Sci.* **2015**, *132*, 41859.
9. Xiao, L.; Sun, D. C.; Niu, T. L.; Yao, Y. W. *Phosphorus Sulfur Silicon Relat. Elem.* **2014**, *189*, 1564.
10. Gu, L. Q.; Chen, G. A.; Yao, Y. W. *Polym. Degrad. Stabil.* **2014**, *108*, 68.
11. Sun, D. C.; Yao, Y. W. *Polym. Degrad. Stabil.* **2011**, *96*, 1720.
12. Chao, P. J.; Li, Y. J.; Gu, X. Y.; Han, D. D.; Jia, X. Q.; Wang, M. Q.; Zhou, T. F.; Wang, T. J. *Polym. Sci. Part A: Polym. Chem.* **2015**, *6*, 2977.
13. Yang, S.; Wang, J.; Huo, S. Q.; Cheng, L. F.; Wang, M. *Polym. Degrad. Stabil.* **2015**, *119*, 251.
14. Yang, S.; Wang, J.; Huo, S. Q.; Wang, M.; Cheng, L. F. *Ind. Eng. Chem. Res.* **2015**, *54*, 7777.
15. Qian, L. J.; Ye, L. J.; Xu, G. Z.; Liu, J.; Guo, J. Q. *Polym. Degrad. Stabil.* **2011**, *96*, 1118.
16. Qian, L. J.; Ye, L. J.; Qiu, Y.; Qu, S. R. *Polymer* **2011**, *52*, 5486.
17. Qian, L. J.; Qiu, Y.; Liu, J.; Xin, F.; Chen, Y. J. *J. Appl. Polym. Sci.* **2014**, *131*, 1.
18. Perret, B.; Schartel, B.; Stöß, K.; Ciesielski, M.; Diederichs, J.; Döring, M.; Krämer, J.; Altstädt, V. *Eur. Polym. J.* **2011**, *47*, 1081.
19. Qian, L. J.; Qiu, Y.; Sun, N.; Xu, M. L.; Xu, G. Z.; Xin, F.; Chen, Y. J. *Polym. Degrad. Stabil.* **2014**, *107*, 98.
20. Yang, X. Y.; Xu, P. Y.; Huan, S. Y. *J. Wuhan Univ. (Nat. Sci. Ed.)* **2001**, *47*, 182.
21. Zhang, W. C.; Li, X. M.; Yang, R. J. *Polym. Degrad. Stabil.* **2011**, *96*, 2167.
22. Sung, J. G.; Li, Y. H.; Sun, X. S. *J. Appl. Polym. Sci.* **2015**, *132*, 41773.
23. Jaillot, F.; Nouailhas, H.; Boutevin, B.; Caillol, S. *Eur. Polym. J.* **2015**, *71*, 248.
24. Deng, J.; Liu, X. Q.; Li, C.; Jiang, Y. H.; Zhu, J. *RSC Adv.* **2015**, *5*, 15930.
25. Liu, S. M.; Chen, J. B.; Zhao, J. Q.; Jiang, Z. J.; Yuan, Y. C. *Polym. Int.* **2015**, *64*, 1182.
26. Harvey, B. G.; Chafin, A. C.; Garrison, M. D.; Cambrea, L. R.; Groshens, T. J. *RSC Adv.* **2015**, *5*, 74712.
27. Lin, C. H. *Polymer* **2004**, *45*, 7911.
28. Spontón, M.; Lligadas, G.; Ronda, J. C.; Galià, M.; Cádiz, V. *Polym. Degrad. Stab.* **2009**, *94*, 1693.
29. Wu, Z. J.; Li, J. L.; Chen, Y. P.; Wang, Z.; Li, S. C. *J. Appl. Polym. Sci.* **2014**, *131*, DOI: 10.1002/app.40848.
30. Wang, X.; Hu, Y.; Song, L.; Xing, W. Y.; Lu, H. D.; Lv, P.; Jie, G. X. *Polymer* **2010**, *51*, 2435.
31. Carja, I. D.; Serbezeanu, D.; Vlad-Bubulac, T.; Hamciuc, C.; Coroaba, A.; Lisa, G.; Guillem Lopez, C.; Fuensanta Soriano, M.; Forrat Perez, V.; Romero Sanchez, M. D. *J. Mater. Chem. A* **2014**, *2*, 16230.

32. Liang, B.; Cao, J.; Hong, X. D.; Wang, C. S. *J. Appl. Polym. Sci.* **2013**, *128*, 2759.
33. Balabanovich, A. I. *Thermochim. Acta* **2005**, *435*, 188.
34. Jiang, W. Z.; Hao, J. W.; Han, Z. D. *Polym. Degrad. Stabil.* **2012**, *97*, 632.
35. Schartel, B.; Perret, B.; Dittrich, B.; Ciesielski, M.; Krämer, J.; Müller, P.; Altstädt, V.; Zang, L.; Döring, M. *Macromol. Mater. Eng.* **2016**, *301*, 9.
36. Wang, Z. Z.; Lv, P.; Hu, Y.; Hu, K. L. *J. Anal. Appl. Pyrolysis* **2009**, *86*, 207.
37. Lv, Q.; Huang, J. Q.; Chen, M. J.; Zhao, J.; Tan, Y.; Chen, L.; Wang, Y. Z. *Ind. Eng. Chem. Res.* **2013**, *52*, 9397.
38. Wang, X.; Hu, Y.; Song, L.; Yang, H. Y.; Xing, W. Y.; Lu, H. D. *Prog. Org. Coat.* **2011**, *71*, 72.
39. Li, K.; Wang, K.; Zhan, M. S.; Xu, W. *Polym. Degrad. Stabil.* **2013**, *98*, 2340.
40. Zahra, Y.; Djouani, F.; Fayolle, B.; Kuntz, M.; Verdu, J. *Prog. Org. Coat.* **2014**, *77*, 380.
41. Zhang, W. C.; Li, X. M.; Fan, H. B.; Yang, R. J. *Polym. Degrad. Stabil.* **2012**, *97*, 2241.
42. Tian, N. N.; Gong, J.; Wen, X.; Yao, K.; Tang, T. *RSC Adv.* **2014**, *4*, 17607.
43. Qian, L. J.; Qiu, Y.; Wang, J. Y.; Xi, W. *Polymer* **2015**, *68*, 262.
44. Gallo, E.; Schartel, B.; Braun, U.; Russo, P.; Acierno, D. *Polym. Adv. Technol.* **2011**, *22*, 2382.
45. Balabanovich, A. I.; Pospiech, D.; Häußler, L.; Harnisch, C.; Döring, M. *J. Anal. Appl. Pyrolysis* **2009**, *86*, 99.
46. Rakotomalala, M.; Wagner, S.; Döring, M. *Materials* **2010**, *3*, 4300.
47. Liu, H.; Wang, X. D.; Wu, D. Z. *Polym. Degrad. Stabil.* **2015**, *118*, 45.
48. Wang, Z.; Wu, W.; Zhong, Y. H.; Ruan, M. Z.; Hui, L. L. *J. Appl. Polym. Sci.* **2015**, *132*, DOI: 10.1002/app.41545.
49. Jiang, S. D.; Bai, Z. M.; Tang, G.; Song, L.; Stec, A. A.; Hull, T. R.; Hu, Y.; Hu, W. Z. *ACS Appl. Mater. Interfaces* **2014**, *6*, 14076.
50. Zhang, Y.; Ni, Y. P.; He, M. X.; Wang, X. L.; Chen, L.; Wang, Y. Z. *Polymer* **2015**, *60*, 50.